Mon. Not. R. astr. Soc. (1984) 209, 401–413

Surface photometry of powerful radio galaxies: their relation to Abell cluster cD galaxies

S. J. Lilly★, I. S. McLean and M. S. Longair *Department of Astronomy, University of Edinburgh, and Royal Observatory, Blackford Hill, Edinburgh EH9 3HJ, United Kingdom*

Received 1984 January 9; in original form 1983 September 23

Summary. Surface brightness profiles of 10 powerful 3C radio galaxies at moderate redshift ($0.06 < z < 0.3$) yield lower values of the structure parameter α than are typically found in first ranked Abell cluster galaxies. This difference has consequences for studies in observational cosmology that mix high-redshift radio galaxies and low-redshift Abell cluster galaxies. Comparisons with earlier qualitative work on lower-redshift radio galaxies suggests that this difference may reflect a change in environment and that it may be related to differences in the radio morphology. A possible mechanism is that the more distant radio galaxies occupy locations which produce lower merging rates of companion galaxies than are found in Abell clusters.

1 Introduction

Ostriker & Tremaine (1975) suggested that the merging of cluster members with the central giant elliptical galaxy is an important evolutionary process in determining the structure and luminosities of first ranked cluster galaxies. The mergers are caused by a loss of orbital energy due to the action of dynamical friction forces. Further theoretical work (e.g. Gunn & Tinsley 1976; Hausman & Ostriker 1978) indicated that, under the assumption of homology, these mergers result in relations between various photometric parameters. These arise because the merger remnant must have the same total mass and binding energy as the initial two galaxies. In particular, there should be a relation between the absolute visual magnitude ($M_{v\gamma}$), measured through an aperture of fixed metric radius γ, and the dimensionless structure parameter α introduced by Gunn & Oke (1975). α_γ is defined to be the slope of the logarithmic growth curve of integrated luminosity with radius evaluated at γ; algebraically this definition of α_γ is exactly the same as twice the ratio of the mean surface brightness at γ to the mean surface brightness inferior to γ.

$$\alpha_\gamma = \left.\frac{d\log L}{d\log r}\right|_\gamma = 2\,\frac{\mathrm{SB}(\gamma)}{\mathrm{SB}_\gamma} \tag{1}$$

The sampling radius, γ, used by, for example, Gunn & Oke (1975) is 19.2 h^{-1} kpc, where

★ Present address: Princeton University Observatory, Peyton Hall, Princeton, New Jersey 08544, USA.

$H_0 = 50\,h$ km s^{-1} Mpc^{-1}. This means that $M_{v\gamma}$ and α_γ measure the properties of the main body of the galaxy and to a large degree exclude the extended envelope that is the defining feature of cD galaxies (Matthews, Morgan & Schmidt 1964). Henceforth in this paper the sampling radius $\gamma = 19.2\,h^{-1}$ kpc will be used and α_γ and $M_{v\gamma}$ will be written as α and M_v.

α is a normalized measure of the surface brightness at a fixed sampling radius, and is hence related to the de Vaucouleurs characteristic radius r_e. For $\alpha > 0.25$, it is found that α varies approximately linearly with $\log r_e$, for a circular galaxy with a de Vaucouleurs profile.

$$\alpha \approx 0.58\,(\log r_e) - 0.18 \qquad (r_e \text{ in kpc}) \tag{2}$$

In the case of non-circular galaxies, α increases slightly with increasing ellipticity at constant r_e. The change in α is not large, and should be less than 10 per cent for galaxies rounder than E4.

Hoessel (1980) analysed the surface brightness profiles and absolute magnitudes of 108 Abell cluster first ranked galaxies, and found a relation between M_v and α. The application of an 'α-correction' to remove this correlation between M_v and α reduced the intrinsic cosmic scatter in the absolute magnitudes of the galaxies from about 0.4 to 0.25 mag. His important observation that 28 per cent of the gE galaxies in his sample have multiple nuclei is probably the most direct evidence that merging does occur in these systems. This work has been extended recently by Schneider, Gunn & Hoessel (1983).

In this paper we report the first results of a project to investigate the values of the α parameter for a sample of giant ellipticals associated with powerful radio sources at moderate redshift ($z < 0.3$). There are several motivations for this study. Firstly, we wish to examine the relationship between the radio galaxies associated with strong radio sources and other giant ellipticals, and in particular the first ranked galaxies in Abell clusters. This is important not only because it may throw light on the radio galaxy phenomenon, but also because several studies of very distant galaxies have compared distant radio galaxies with nearby Abell cluster galaxies under the assumption that they are essentially the same sort of galaxy. Secondly, if α can be taken as an indicator of the degree of dynamical evolution that has taken place, it is of interest to assess the importance of this process for radio galaxies. Such information may be relevant to the question of the links between the evolutionary processes that occur in the host galaxies and the bulk cosmological evolution of the radio source population (e.g. Longair 1966; Peacock & Gull 1981). In addition, the amount of dynamical evolution that has taken place has to be taken into account in interpreting the infrared (K, z) Hubble relation for radio galaxies (Lilly & Longair 1982, in preparation 1984). Thirdly, a study of the range of growth curves exhibited by these radio galaxies gives direct information on the corrections that need to be applied to produce optical to infrared colours such as $(V-K)$ and metric magnitudes from the single aperture infrared photometry of Lilly & Longair (1982, in preparation 1984). Finally, in this study the (M_v, α) relation is analysed for a sample of massive ellipticals selected without direct regard to their cluster environment.

Section 2 describes the acquisition and reduction of the CCD data. In Section 3, we discuss the location of the radio galaxies on the (M_v, α) diagram, while Section 4 summarizes our conclusions.

2 The data

Ten radio galaxies have been observed so far for this project. They were selected from the 3CR 'complete sample' of Laing, Riley & Longair (1983) to be Fanaroff-Riley Class II sources (the 'classical doubles', Fanaroff & Riley 1974) with $z < 0.3$ and declination $\delta < 55°$. We have not observed any broad line radio galaxies (BLRG) since they are usually associated

with N-type morphology. Their highly active nuclei will distort the surface brightness profiles measured for the galaxies. Although the 10 galaxies observed do not form a statistically complete sample, it is none the less believed that they comprise a small but representative sample of powerful FR II radio galaxies. Such a statistically complete sample may however be defined based on the Jenkins, Pooley & Riley (1977) 166-source sample with the further selection criteria in right ascension (between 09 and 18 hr), redshift ($0.05 < z < 0.30$), and excluding 3C 234 (a BLRG, Grandi & Osterbrock 1978) and 3Cs 288, 310, 315 (which are FR I sources, Laing *et al.* 1983). Apart from 3C 33 which was observed in the autumn, the remaining nine radio galaxies observed in this programme form 75 per cent of this well-defined sample. The three radio galaxies in this well-defined sample that were not observed here (3Cs 303, 321, 326) are quite unremarkable and were omitted randomly. The FR II type of radio sources are of particular interest for two related reasons. For extended radio sources, they are the type of radio source that is responsible for the bulk cosmological evolution of the radio source population. In addition, most of the high redshift 3CR radio galaxies studied at redshifts of about unity are associated with this type of radio source.

The galaxies observed are listed in Table 1. Their radio structures have a range of linear sizes from $48h^{-1}$ kpc (3C 277.3) to $5.7h^{-1}$ Mpc (the giant 3C 236) but are typically a few hundred kpc in extent. They are evenly distributed in 'quality' of double (Longair & Riley 1979) having approximately equal numbers of 'good', 'doubtful', and one-sided hotspot sources. The apparent magnitudes of these galaxies are listed by Laing *et al.* (1983).

Surface photometry for these galaxies was obtained using the Royal Observatory Edinburgh CCD Imaging/Spectropolarimeter System (McLean *et al.*, 1981). The CCD employed was a thinned backside illuminated RCA device with 30 μm pixels in a 512×320 array format. Readout noise was approximately 70 electrons. Except for 3C 33, which was observed with the University of Arizona Observatory's 1.54-m telescope in 1981 November, all the galaxies were observed with the CCD camera mounted on the 3.8-m United Kingdom Infrared Telescope on Mauna Kea in 1982 April. These latter observations were made in conditions of good seeing but poor and varying atmospheric transparency. The exposure times varied between 5 and 15 min. The UAO 1.54 m and UKIRT gave plate scales of 0.75 and 0.41 arcsec per pixel respectively. All the galaxies were observed through a red interference filter with half peak transmissions at 7200 Å and 7980 Å. 3C 284 and 3C 349 were also observed through a V filter (4800 Å–5730 Å). The seeing, defined as the FWHM of a Gaussian fitted to the stellar profiles, varied slightly between exposures but was less than 1.5 arcsec for all images except that of 3C 219 for which it was 1.7 arcsec.

The raw CCD exposures were reduced in the following way. First, an electronic bias

Table 1. The data for the radio galaxies.

3CR	z	α_{obs}	σ/γ	α_o	$M_{v\gamma}$
33	0.060	0.32 ± 0.02	0.07	0.31 ± 0.02	-22.58
285	0.079	0.34 ± 0.02	0.07	0.33 ± 0.02	-22.45
277.3	0.086	0.39 ± 0.01	0.08	0.38 ± 0.01	-22.63
236	0.099	0.49 ± 0.02	0.09	0.48 ± 0.02	-22.88
223	0.137	0.37 ± 0.02	0.11	0.36 ± 0.02	-22.65
219	0.174	0.43 ± 0.02	0.16	0.41 ± 0.02	-23.05
319	0.192	0.19 ± 0.08	0.13	0.18 ± 0.08	-22.15
349	0.205	0.37 ± 0.05	0.17	0.35 ± 0.05	-22.05
284	0.239	0.48 ± 0.03	0.15	0.46 ± 0.03	-22.95
300	0.270	0.24 ± 0.07	0.17	0.22 ± 0.07	-22.07

offset, determined regularly throughout the night by repeated readouts of the unexposed chip, and a dark-current signal, found by long exposures at the start of each night's work with the camera shutter closed, were subtracted from each exposure. The resulting image was then divided by a flat field exposure (similarly bias subtracted) that had been obtained by observing the twilight sky. After these standard operations had been carried out, two further cosmetic defects were removed as follows. The first was a form of non-linearity in the response of the RCA CCD which resulted in certain columns of the chip being systematically less sensitive. This effect was only of the order of 1–2 per cent and it was found that a single multiplicative correction applied to all the pixels of each affected column was sufficient to remove it. An iterative algorithm was developed to apply a correction to each column such that the mean sky background was flat across each row of pixels. The second defect manifested itself as horizontal rows of increased charge every 16 rows and was caused by a small change in the value of the bias offset following interruptions in the readout process during which the CCD output is written to disc. Because the bias level was very small compared with the mean background level in the astronomical images, this defect could be removed by applying a single additive correction to each affected row, again with the requirement that the mean sky background up a column be constant. The application of these two processes resulted in extremely clean images. No fringes were seen on these images. This was because the red filter used avoided the strongest sky lines and because the particular RCA chip used as detector was not as thin as most.

The derivation of the α-parameter was carried out in the following manner. The centre of the galactic image was found by fitting a Gaussian profile to the central regions. Stars, faint galaxies and cosmic rays were then removed from around the image of the radio galaxy. If the object to be removed lay more than 2γ from the centre of the radio galaxy the pixel values were replaced by a sky value that had been produced by the defect removal algorithms described above plus a Gaussian noise component. If the object was closer than this, the pixel values were replaced by those found by a 180° rotation about the radio galaxy centre, interpolating where necessary. An improved value of the sky background was then determined, with an estimate of its uncertainty, by fitting a Gaussian to the top of the histogram of the distribution of all pixel values in the annulus of inner and outer radii 2γ and 4γ centred on the radio galaxy. The sky at these large radii (about $60h^{-1}$ kpc at the galaxy) may still be slightly contaminated by the outermost parts of the galaxy. The size of the effect on α should be small, however, and should be independent of magnitude and redshift. A de Vaucouleurs $r^{1/4}$ surface brightness distribution of appropriate r_e has a surface brightness at 3γ that is a factor of 20 less than that at γ, while $60h^{-1}$ kpc is in any case close to the cut-off radius. A contamination in the sky level equivalent to 5 per cent of the galactic surface brightness at γ leads to a 5 per cent error in α in the sense that the measured value of α is too low. The accurate sky value was then subtracted from every pixel in the image.

An empirical growth curve was constructed by plotting the cumulative galactic flux density as a function of radial distance. Digitization is important for the first few pixels but is negligible at γ, typically about 10 pixels radius. This empirical growth curve extended out to 2.0γ. A sixth order polynomial was then fitted to this curve for two reasons. The first reason was to smooth out small variations in the growth curve due to noise in each pixel, and secondly to aid in the analytic calculation of α and its upper and lower bounds caused by the uncertainty in the sky background level. The growth curve of 3C 223, a typical member of the sample with a redshift of 0.137, is shown in Fig. 1a. The solid line is the fitted polynomial, while the two dashed lines indicate the polynomial growth curves that are derived with different sky values assumed. The two dashed lines correspond to rather different assumptions about the background estimate and corresponding to three times the formal

uncertainty in the background. The sampling radius γ is shown. This approach is slightly different from that taken by Hoessel (1980), who derived α from the parameters of a fitted Hubble law. Our fit is essentially free-form. The most important consequence of this is that at small α (less than about 0.4) α may be slightly overestimated by the Hubble law fit. This is illustrated by fig. 8 of Schneider *et al.* (1983) which shows $\alpha(r)$ for de Vaucouleurs and Hubble surface brightness profiles.

As a check on the growth curve and the assumed values of the background intensity, the three polynomials were plotted in the form of curves of surface brightness in magnitudes relative to sky, against the radius in pixels to one-quarter power. A de Vaucouleurs $r^{1/4}$ distribution is a straight line on such a plot, although the radius used here is a circular radius and not an effective radius (the geometric mean of the semi-major and semi-minor axes). Fig. 1b shows this diagram for 3C 233.

It can be seen that in all three cases, the surface brightness distribution follow closely the $r^{1/4}$ law, even out to the lowest isophotes which are most sensitive to uncertainties in the background. The observed values of α determined at γ for all the galaxies are tabulated in the third column of Table 1.

A correction must be applied to α to allow for the effects of seeing. Because α is a measure of the surface brightness at a relatively large radius compared with the mean surface brightness within that radius the effect of seeing is not as critical as when one is attempting to measure nuclear parameters such as the nuclear core radius. Fig. 2 shows the effect of degrading various model galactic profiles with different intrinsic α's (essentially different core radii) with Gaussian seeing profiles of standard deviation σ. Provided that σ is sufficiently smaller than the sampling radius γ, $\sigma/\gamma < 0.20$, the corrections to α are small and may safely be applied. σ/γ was less than 0.2 for even the most distant galaxies in our study, and the seeing correction applied to α was in all cases less than 0.025. σ/γ and the corrected α are listed in Table 1.

Absolute magnitudes in the V passband for the six nearest radio galaxies were derived from the fully corrected V photometric data of Sandage (1972) since our CCD data for these objects were not obtained in photometric conditions. A small correction was applied so that the magnitudes are appropriate for a $q_0 = 0.5$ cosmology, and an aperture correction, derived from the CCD surface photometry, was included to derive M_v. For two of the remaining galaxies (3C 284 and 3C 349) our CCD data was of photometric quality, and absolute magnitudes have been derived from these exposures. They were reduced using the photometric system outlined by Lilly, Langair & McLean (1983), and have an uncertainty of about 15 per cent. For the remaining two galaxies, we have estimated a V absolute magnitude from our K (2.2 μm) photometry (Lilly & Longair1982;, in preparation 1984) and non-photometric CCD data. The uncertainties in these last two galaxies are therefore quite large, but none of our conclusions depend on the precise magnitudes of these galaxies. The final column in Table 1 lists the adopted absolute magnitudes.

In order to ensure consistency with the large data set of Hoessel (1980), an exposure of the central cD in Abell 104 was taken with the UAO 1.54-m telescope in 1981 November. This was reduced and analysed in an identical way to the radio galaxies. The corrected value of α was 0.71 ± 0.01 in good agreement with Hoessel's 0.70 ± 0.03.

3 Discussion

Fig. 3 shows the location of the ten 3C radio galaxies in the (M_v, α) diagram. They are plotted as solid circles with error bars. Also shown are the 108 Abell first ranked cluster galaxies from Hoessel (1980) (open circles), 84 other Abell first ranked cluster galaxies

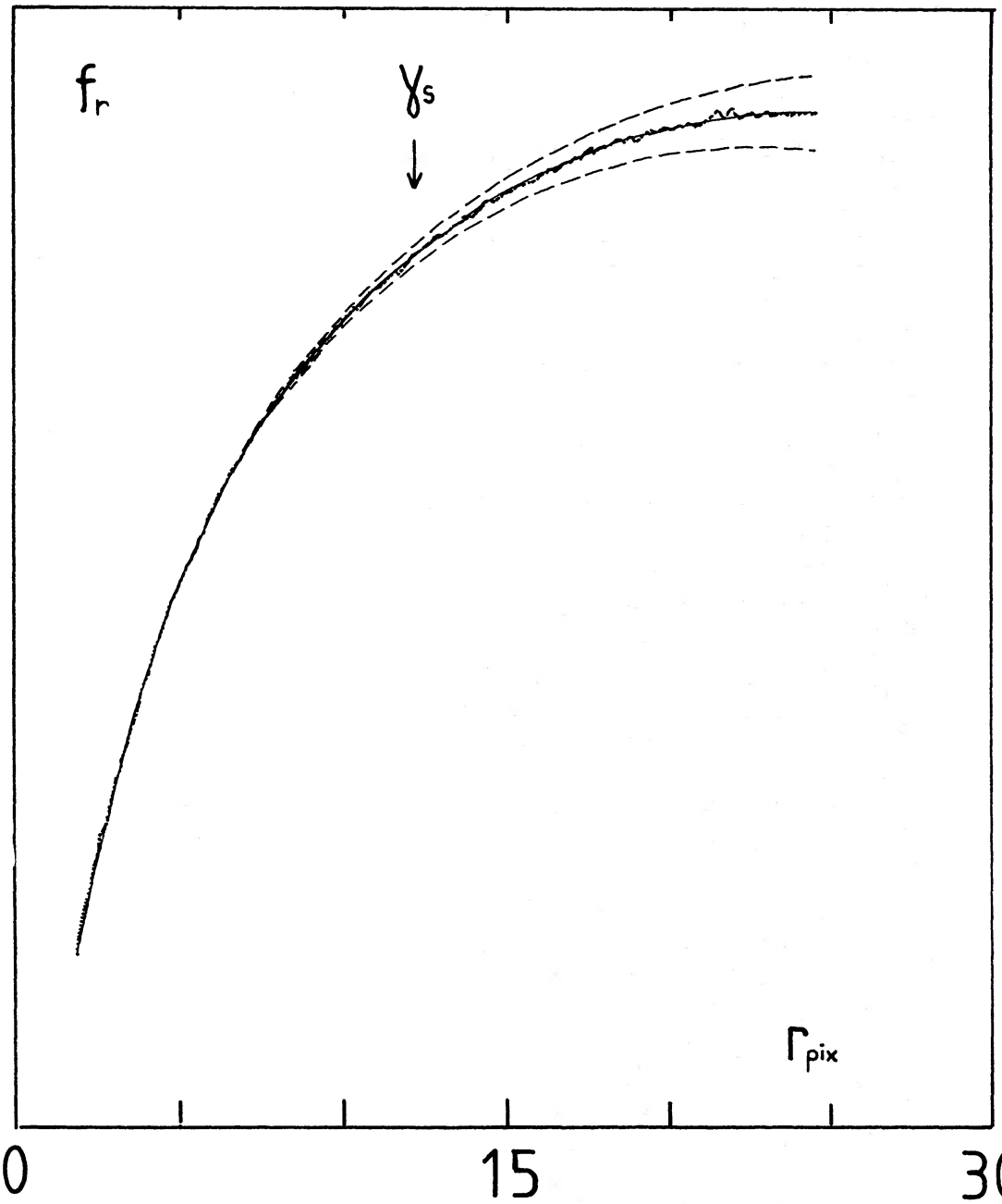

Figure 1(a). The growth curve of enclosed flux density as a function of aperture radius for 3C 223 ($z = 0.137$). The vertical scale is linear in flux density. The sampling radius γ is shown. The solid line is a sixth order polynomial fitted to the data and the two dashed lines represent the growth curves derived by taking extreme values for the sky background.

(Schneider *et al.* 1983), (open squares) and the nine first ranked cluster galaxies from the poor clusters of Morgan, Kayser & White (1975, MKW) and Albert, White & Morgan (1977, AMW) studied by Thuan & Romanishin (1981) (plotted as asterisks). The parameters for the Schneider *et al.* (1983) galaxies have been derived from the values of Reduced Absolute Magnitude (RAM) and log r_e given by them while those for the MKW and AMW clusters were derived from the values of Absolute Magnitude and r_e given by Thuan & Romanishin (1981). The measurements of α in the first two studies were based on r CCD images. The slightly shorter effective wavelength of their r filter is compensated for by the generally higher redshifts of the present study. These measurements are therefore directly comparable to

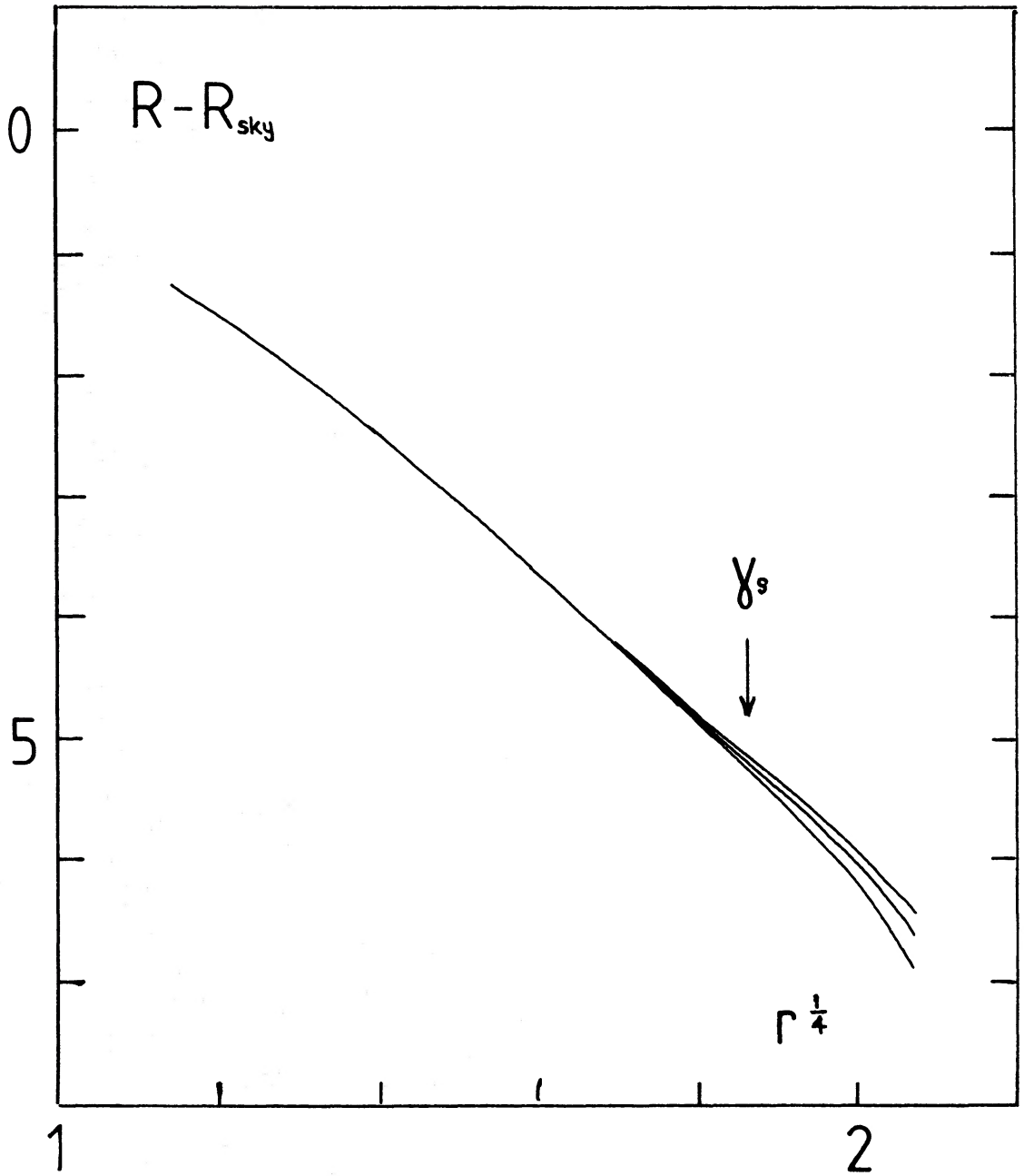

Figure 1(b). The variation of mean surface brightness relative to the sky background with radius to the one quarter power for 3C 223. A de Vaucouleurs $r^{1/4}$ law is a straight line on this diagram. The three curves represent the three polynomial growth curves shown in (a).

those presented in this paper. Thuan & Romanishin (1981) used both g and r filters. However, in those galaxies for which they had images in both colours they found no evidence for colour gradients. The solid line marked K77 represents the relation between M_v and α for normal elliptical galaxies derived from the relation between B_e and r_e found by Kormendy (1977). The standard deviation of the scatter about this mean line is 0.6 mag. The dashed line ($k = 1$) indicates one of the predicted evolutionary tracks for homologous mergers (Hausman & Ostriker 1978; Hoessel 1980), and will be discussed in Section 3.2.

Two things are evident from Fig. 3. Firstly, all the radio galaxies lie within the range of (M_v, α) combinations occupied by the normal elliptical galaxies observed by Kormendy (1977). The seven most luminous galaxies have (M_v, α) parameters similar to those found in

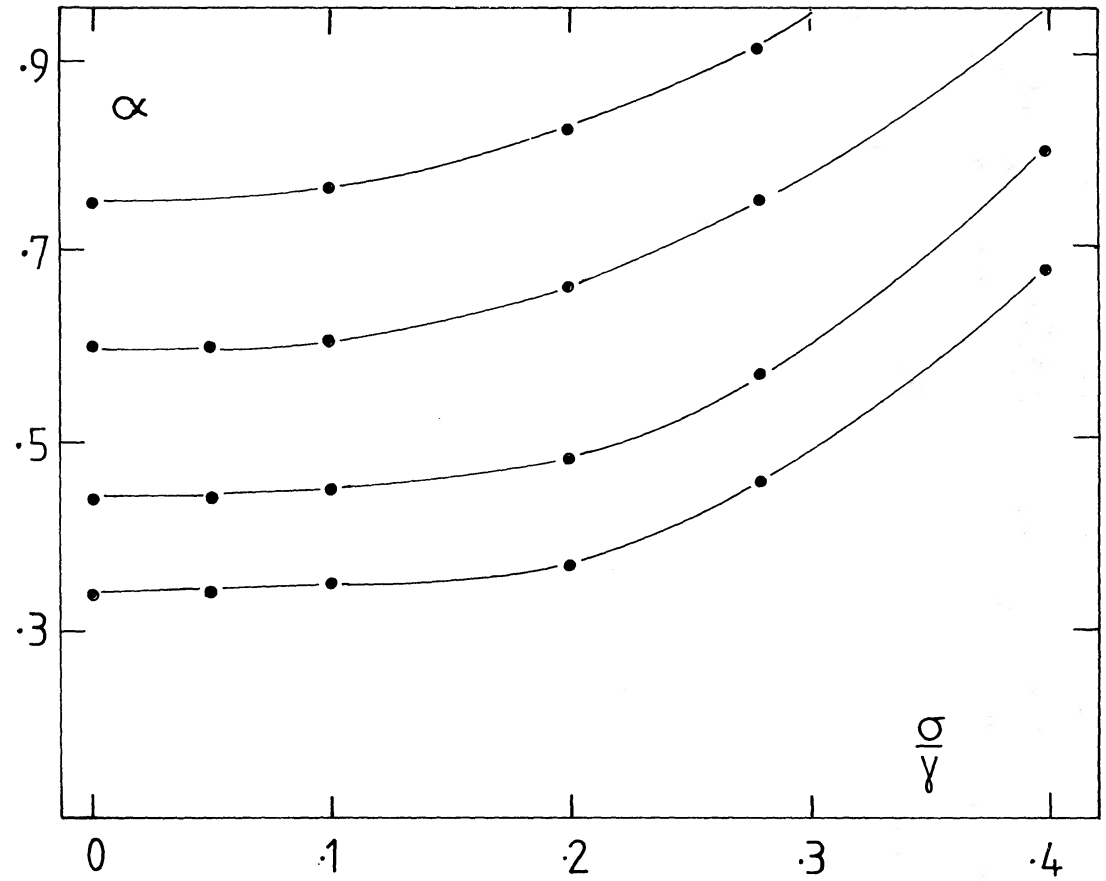

Figure 2. The effect of seeing in increasing the observed value of α. σ/γ is the ratio of the standard deviation of the seeing Gaussian to the sampling radius. The four lines respresent four model galaxies with different intrinsic α.

some Abell cluster galaxies. This implies that the radio galaxies do not have unusual surface brightness distributions. Since the colours of these narrow line radio galaxies are not anomalous (e.g. Sandage 1972; Lilly & Longair 1982, in preparation 1984) this implies that in the majority of cases one cannot distinguish photometrically between giant ellipticals that have or do not have powerful double radio sources associated with them.

The second result is more interesting and is the subject of the remainder of this discussion; the radio galaxies that we have studied do not span the same range of α as the Abell cluster galaxies, and in particular do not have large values of α. The radio galaxies have a mean value of 0.35 with a dispersion of 0.08. This is significantly lower than the mean value of α of the Abell cluster galaxies which Hoessel finds to be 0.49 (1980) and which is 0.70 from the richer cluster sample of Schneider *et al.* (1983). Indeed, none of the radio galaxies has a value of α greater than either the mean or the median (0.48) of the Hoessel Abell sample. Even if attention is restricted to the Richness Class 0 or Bautz-Morgan Class III Abell cluster galaxies of Hoessel (1980), the mean α's (0.41 and 0.47 respectively) are still significantly higher than that of the radio galaxies.

These 10 radio galaxies are clearly host to an active nucleus and it is important to note the effect of adding an unresolved nuclear component to an otherwise normal galaxy. Remembering the definition of α in terms of the ratio of surface brightnesses, the addition of, say, a 20 per cent nuclear component in the R band will decrease α by about 20 per cent (about 0.01) while it will increase the absolute magnitude at V by about 0.2 mag, depending on the precise relative spectral indices of the nuclear component and the starlight. This

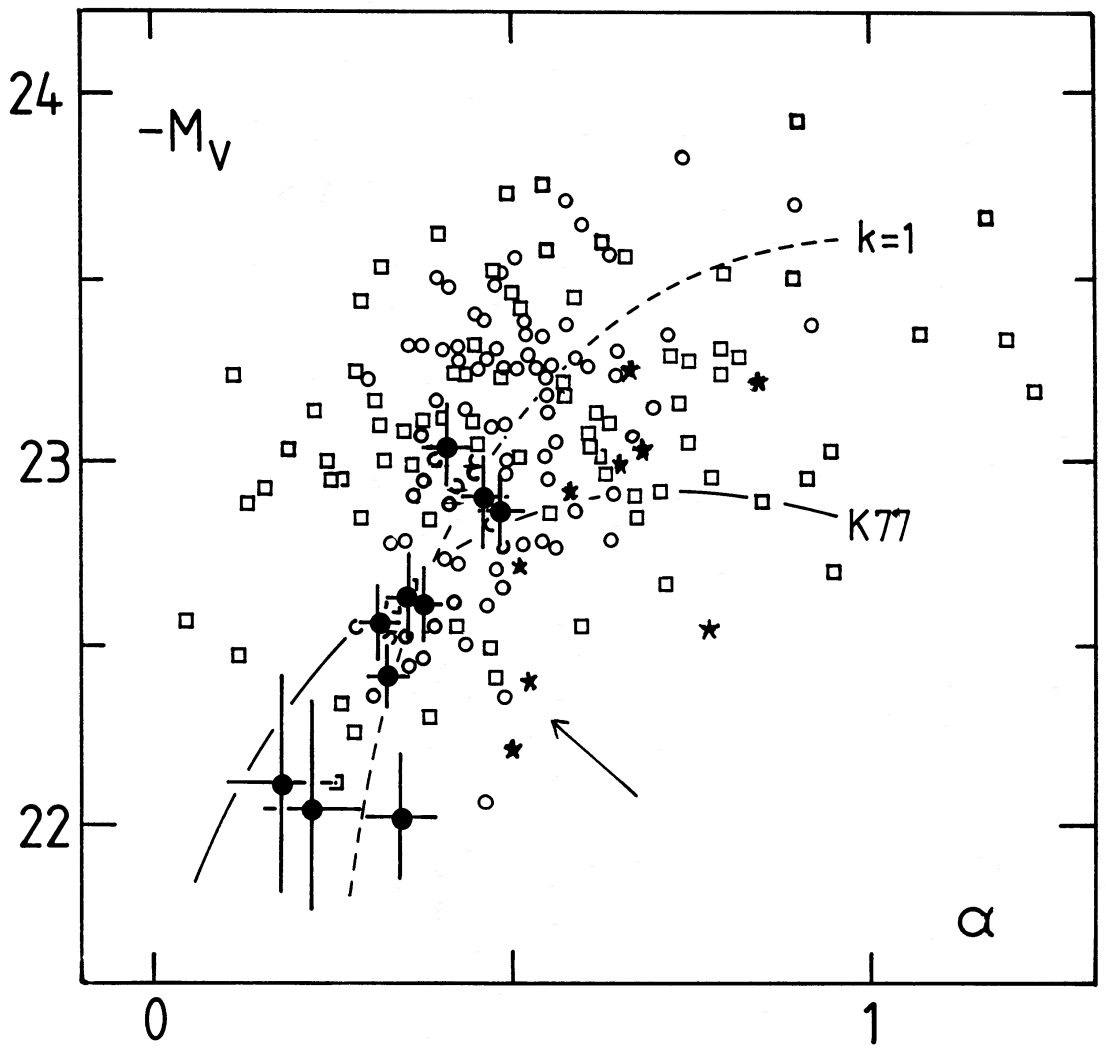

Figure 3. The (M_V, α) diagram for massive elliptical galaxies. Ten 3CR galaxies are shown as filled circles with error bars. Data for Abell cluster galaxies is taken from Hoessel (1980) (○), and Schneider *et al.* (1983) (□). That for the poor AMW and MKW cluster galaxies is derived from Thuan & Romanishin (1981) and is represented by (*). The solid curve represents the Kormendy (1977) relation between surface brightness and effective radius, while the dashed curve is an evolutionary track produced by homologous mergers. The vector shows the effect of adding an unresolved nuclear component whose luminosity is 20 per cent of the galaxy metric luminosity.

vector is shown on Fig. 3, and it is clear that this cannot be the cause either of the difference between Abell cluster galaxies and 3C radio galaxies, or of the relation exhibited by the radio galaxies alone. Furthermore since all the radio galaxies lie close to the mean Kormendy relation, it is unlikely that they have substantial unresolved nuclear components. Relations were searched for between α and various radio parameters such as linear size, luminosity, spectral index, and 'quality' of double source. No relations were found although the sample is of course very small.

3.1 THE DIFFERENCE BETWEEN 3CR RADIO GALAXIES AND ABELL CLUSTER GALAXIES

The first question that arises is why the radio galaxies avoid the upper right quadrant of Fig. 3. It is well known that radio activity generally occurs in more luminous galaxies

(Sandage 1972, Fanti & Perola 1977) and yet these most powerful radio sources are not in the most luminous galaxies known, namely those in the upper right quadrant of Fig. 3. The explanation may lie either in some intrinsic property of the galaxy related to its mass, or equally plausibly, to some property of the local environment. A different environment is likely to affect the radio power and morphology of the radio source and may also affect the mass and structure of the giant elliptical, particularly if merging has taken place.

It is of interest to note the possible difference between the results of this work and the qualitative investigations of Matthews *et al.* (1964). The cD-type of optical morphology was introduced by Matthews *et al.* (1964) in order to describe the appearance of radio galaxies at somewhat lower redshifts, and was subsequently found to be appropriate to first ranked Abell cluster galaxies and also to the first ranked cluster galaxies of the poorer AMW and MKW clusters. These latter galaxies have relatively high values of the α-parameter (Thuan & Romanishin 1981) and it is quite plausible that the low redshift radio galaxies classified as cD-type by Matthews *et al.* (1964) do have higher values of α than the radio galaxies that we have studied here. Such a difference, if confirmed, would be interesting, since the difference in redshift between the two samples results in a difference of radio morphology as well as a difference in luminosity, because radio morphology is related to radio luminosity (Fanaroff & Riley 1974). Consequently 70 per cent of the radio galaxies classified as cD-type by Matthews *et al.* (1964) have Fanaroff–Riley I radio structure, whereas all of the radio galaxies studied in the present paper have FR II structure.

However, we do note that there is at least one exception to this idea that there is a relation between the optical and radio morphology. Spinrad & Stauffer (1982) have presented photographic surface photometry of 3C 405 (Cyg A) which indicates that this galaxy has both a high α (about 0.8) and a high total luminosity, even though it has classical double radio morphology. The results of this paper should be extended to larger statistical samples of radio galaxies.

In addition, the results of Longair & Seldner (1979) are relevant. They investigated the amplitudes of the spatial cross-correlation function of galaxies around radio galaxies at redshifts less than 0.1, compared to the amplitude around randomly selected galaxies. Their statistic B_{gg}^{*}/B_{gg} is the ratio of these amplitudes, and for Abell cluster galaxies, ranges from about 13 for Richness Class 2 clusters to about 4.5 for Richness Class 0 clusters. For the weakest sources, with radio luminosities only 10 to 1000 times that of our own galaxy they found $\langle B_{gg}^{*}/B_{gg}\rangle$ to be essentially unity, which implies that these galaxies are a random sample of the total galaxy population. On the other hand, the more powerful sources, classed as 'radio galaxies' and associated with nuclear activity, were found to have $\langle B_{gg}^{*}/B_{gg}\rangle$ about 5, indicating that they were preferentially found in clusters and groups of galaxies comparable to Abell clusters. However, their surprising result was that the eight 'good classical double' FR II sources in their sample had $\langle B_{gg}^{*}/B_{gg}\rangle \sim 1$, which indicates that these most powerful radio sources are not found in the same cluster environments as the weaker radio galaxies which have $\langle B_{gg}^{*}/B_{gg}\rangle \sim 5$. This is consistent with the present results since the values of α for Abell cluster galaxies are correlated weakly with the cluster richness (Hoessel 1980). Note however, that the 'poor' AMW and MKW cluster galaxies do have relatively high values of α, and occupy a distinctly different area on the (M_v, α) diagram from the radio galaxies.

The location of powerful 3C galaxies on the (M_v, α) diagram and the results of Longair & Seldner (1979) indicate that the radio galaxies studied here are not the same sort of galaxy as the Abell cluster cD ellipticals. This suggests that studies of the evolution of massive elliptical galaxies that use samples of galaxies that are a mixture of first ranked Abell cluster galaxies at low redshift and 3C radio galaxies at high redshift [e.g. the Hubble diagram of Lebofsky (1981) and the (Θ–z) relation of Djorgovski & Spinrad (1981)] may give mislead-

ing results if this difference between first ranked Abell cluster galaxies and powerful radio galaxies is maintained out to $z \sim 1$. This possibility is supported by the work of Djorgovski & Spinrad (1981) who have measured quite low values of α in a small sample of radio galaxies with $0.5 < z < 1.2$. We note, however, two reasons for studying this problem in more detail for radio galaxies with larger redshifts. Firstly, for some years there has been speculation that the environments of quasars may be different at high redshift from those at low redshift (e.g. Stocke & Perrenod 1981). Secondly, we are aware that there are at least two high redshift 3C radio galaxies with $\alpha > 0.7$, these being 3C 34 and 3C 295.

An attractive origin for the difference in α's of the radio galaxies and Abell cluster galaxies is a difference in the number of mergers that have taken place, especially as merging has been proposed as a contributing cause of the (M_v, α) correlation found in the Abell sample by Hoessel (1980). This mechanism could link the optical morphology to the local environment of the radio galaxy.

3.2 THE (M_v, α) DIAGRAM AS AN INDICATOR OF MERGING

Direct evidence for merging in the first ranked ellipticals in clusters comes from Hoessel's observation that 28 per cent of his sample have multiple nuclei. The remainder of the evidence in his paper is based on the (M_v, α) diagram.

If the characteristic radius of the merger remnant increases as the k^{th} power of its mass, $r \propto m^k$, then, in the homologous merging of two galaxies, the case $k = 1$ applies to mergers of galaxies of comparable mass while $k = 2$ applies to mergers of galaxies with very different masses (Gunn & Tinsley 1976; Hoessel 1980). This difference arises because in the former case the specific binding energy remains constant while in the latter the total binding energy remains unchanged. These relations between radius and mass (and hence luminosity) result in different predicted relations in the (M_v, α) diagram. The $k = 1$ curve is shown in Fig. 3, normalized as in Hoessel (1980). As the cannibal galaxy grows it moves to the right in Fig. 3.

The Abell cluster data appear to follow, with large scatter, the $k = 1$ line (Hoessel 1980), as predicted on dynamical grounds (Hausman & Ostriker 1978). α increases with decreasing Bautz–Morgan class, and, less clearly, with increasing richness. A dependence on BM class is important because BM class is often interpreted as indicating the degree of dynamical evolution that has taken place. The theoretical dependence of the merging rate on cluster depends on the inter-relations of cluster size, velocity dispersion and central density. The multiple nuclei systems have higher mean luminosities and higher mean α's than the remainder of the sample. Estimates of the number of mergers that have taken place from these differences are consistent with theoretical predictions of the merging rates, as is the fraction of multiple systems seen.

The poor cluster galaxies of AMW and MKW have relatively high α, and this has been interpreted by Thuan & Romanishin (1981) as being caused by a higher merging rate in these poor systems because of the low velocity dispersion of these clusters. AMW and MKW noted that the hierarchical morphologies of these poor clusters closely resemble those of BM class I clusters which are generally thought to be the most evolved systems. The above arguments suggest that merging is an important factor in both rich Abell clusters and the poor clusters.

On the other hand, Kormendy (1977) has found that a correlation exists between the de Vaucouleurs' parameters B_e and r_e for non-cD ellipticals. Assuming a constant M/L ratio this corresponds to the case $k = 1.45$, and the normalization is such that the extrapolation of this relation on the (M_v, α) plane is also a reasonable fit to the data (see Fig. 3). In other words, the observed (M_v, α) relation in Abell cluster galaxies (Hoessel 1980) could be caused by the, as yet unknown, process producing the Kormendy relation in non-cD galaxies. Furthermore

the assumption of homology in the merging process is not borne out in N-body simulations of encounters between galaxies (White 1978).

In summary, while there is some evidence that α is a measure of the degree of merging that has taken place it cannot be regarded as the only means of producing an M_v-α-correlation. If it is correct, however, then we can say that the low α's of the radio galaxies imply that this evolutionary process may not be important in the Hubble diagram for radio sources. A correction to M_v for cannibalism due to an increase in luminosity with time is probably not appropriate since the nearest members of the sample, and hence the oldest, are in a relatively unevolved state.

The inferred lack of dynamical evolution of the radio galaxies compared with both Abell clusters and the poorer AMW and MKW clusters may be related to the low density of surrounding galaxies found by Longair & Seldner (1979). The poor clusters of AMW and MKW have a high central density on account of their low velocity dispersion.

It should be stressed that this statement on the lack of merging refers to evolution over cosmological time-scales only. We cannot rule out on the basis of α that a single merger for instance could have occurred relatively recently, perhaps to trigger the nuclear activity. Nevertheless, we do not see any evidence for this having happened (e.g. multiple nuclei) on our CCD exposures.

4. Summary

Studies of the photometric parameters of 10 powerful 3C radio galaxies have indicated that these systems have, in the mean, lower luminosities and lower values of the structure parameter, α, than both Abell first ranked cluster galaxies and the brightest members of AMW and MKW poor clusters. These differences may be caused by the different environments indicated by recent studies of the clustering of galaxies around the radio galaxies. The different environments may also be reflected in differences inferred from earlier studies at lower redshifts of radio sources with different radio morphologies. The environment can affect the luminosities and α by producing different rates of mergers with nearby galaxies, the radio galaxies occupying locations where little merging has taken place.

The difference between the average properties of first ranked Abell cluster galaxies and the 3C radio galaxies may have consequences for studies in observational cosmology that mix observations of Abell cluster galaxies at low redshift with those of radio galaxies at higher redshift. A lack of dynamical evolution would imply that the dominant evolutionary process in the radio galaxy Hubble diagram is that due to the evolution in the stellar population.

Acknowledgments

We would like to thank the Technology Unit of the Royal Observatory Edinburgh for support of the CCD camera, and our colleagues in Hawaii who prepared UKIRT for use as an optical telescope. It is a pleasure to acknowledge the University of Arizona for allocation of telescope time, and Professor J. P. Ostriker for an interesting comment. SJL thanks the SERC for a Research Studentship.

References

Albert, C. E., White, R. A. & Morgan, W. W., 1977. *Astrophys. J.*, **211**, 309.
Djorgovski, S. & Spinrad, H., 1981. *Astrophys. J.*, **251**, 417.
Fanaroff, B. L. & Riley, J. M., 1974. *Mon. Not. Roy. astr. Soc.*, **167**, 31P.

Fanti, R., Perola, G. C., 1977. *Radio Astronomy and Cosmology, IAU Symp. 74,* p. 171, ed. Jauncey, D. L., Reidel, Dordrecht-Holland.
Grandi, S. A. & Osterbrock, D. E., 1978. *Astrophys. J.,* **220,** 783.
Gunn, J. E. & Oke, J. B., 1975. *Astrophys. J.,* **195,** 255.
Gunn, J. E. & Tinsley, B. M., 1976. *Astrophys. J.,* **210,** 1.
Hausman, M. A. & Ostriker, J. P., 1978. *Astrophys. J.,* **224,** 320.
Hoessel, J. G., 1980. *Astrophys. J.,* **241,** 493.
Jenkins, C. R., Pooley, G. G. & Riley, J. M., 1977. *Mem. R. astr. Soc.,* **84,** 61.
Kormendy, J., 1977. *Astrophys. J.,* **218,** 333.
Laing, R. A., Riley, J. M. & Longair, M. S., 1983. *Mon. Not. R. astr. Soc.,* **204,** 151.
Lilly, S. J. & Longair, M. S., 1982. *Mon. Not. R. astr. Soc.,* **199,** 1053.
Lilly, S. J., Longair, M. S. & McLean, I. S., 1983. *Nature,* **301,** 488.
Lebofsky, M. J., 1981. *Astrophys. J.,* **245,** L59.
Longair, M. S., 1966. *Mon. Not. R. astr. Soc.,* **133,** 421.
Longair, M. S. & Riley, J. M., 1979. *Mon. Not. R. astr. Soc.,* **188,** 625.
Longair, M. S. & Seldner, M., 1979. *Mon. Not. R. astr. Soc.,* **189,** 433.
McLean, I. S., Cormack, W. A., Herd, J. T. & Aspin, C., 1981. *Proc. Soc. photo-opt. Instrum. Engng.,* **290,** 155.
Matthews, T. A., Morgan, W. W. & Schmidt, M., 1964. *Astrophys. J.,* **140,** 35.
Morgan, W. W., Kayser, S. & White, R. A., 1975. *Astrophys. J.,* **199,** 545.
Ostriker, J. P. & Tremaine, S. D., 1975. *Astrophys. J.,* **202,** L133.
Peacock, J. A. & Gull, S. F., 1981. *Mon. Not. R. astr. Soc.,* **196,** 611.
Sandage, A., 1972. *Astrophys. J.,* **178,** 25.
Schneider, D. P., Gunn, J. E. & Hoessel, J. G., 1983. *Astrophys. J.,* **268,** 476.
Spinrad, H. & Stauffer, J. R., 1982. *Mon. Not. R. astr. Soc.,* **200,** 153.
Stocke, J. T. & Perrenod, S. C., 1981. *Astrophys. J.,* **245,** 375.
Thuan, X. T. & Romanishin, W., 1981. *Astrophys. J.,* **248,** 439.
White, S. D. M., 1978. *Mon. Not. R. astr. Soc.,* **184,** 185.